TECHNICAL SPECIFICATION

ISO/TS 6336-21

First edition
2017-11

Calculation of load capacity of spur and helical gears —

Part 21: Calculation of scuffing load capacity (also applicable to bevel and hypoid gears) — Integral temperature method

Calcul de la capacité de charge des engrenages cylindriques à dentures droite et hélicoïdale —

Partie 21: Calcul de la capacité de charge au grippage (applicable également aux engrenages conique et hypoïde) - Méthode de la température intégrale

Reference number
ISO/TS 6336-21:2017(E)

ISO copyright office
Ch. de Blandonnet 8 • CP 401
CH-1214 Vernier, Geneva, Switzerland
Tel. +41 22 749 01 11
Fax +41 22 749 09 47
copyright@iso.org
www.iso.org

Contents

Page

Foreword

ISO (the International Organization for Standardization) is a worldwide federation of national standards bodies (ISO member bodies). The work of preparing International Standards is normally carried out through ISO technical committees. Each member body interested in a subject for which a technical committee has been established has the right to be represented on that committee. International organizations, governmental and non-governmental, in liaison with ISO, also take part in the work. ISO collaborates closely with the International Electrotechnical Commission (IEC) on all matters of electrotechnical standardization.

The procedures used to develop this document and those intended for its further maintenance are described in the ISO/IEC Directives, Part 1. In particular the different approval criteria needed for the different types of ISO documents should be noted. This document was drafted in accordance with the editorial rules of the ISO/IEC Directives, Part 2 (see www.iso.org/directives).

Attention is drawn to the possibility that some of the elements of this document may be the subject of patent rights. ISO shall not be held responsible for identifying any or all such patent rights. Details of any patent rights identified during the development of the document will be in the Introduction and/or on the ISO list of patent declarations received (see www.iso.org/patents).

Any trade name used in this document is information given for the convenience of users and does not constitute an endorsement.

For an explanation on the voluntary nature of standards, the meaning of ISO specific terms and expressions related to conformity assessment, as well as information about ISO's adherence to the World Trade Organization (WTO) principles in the Technical Barriers to Trade (TBT) see the following URL: www.iso.org/iso/foreword.html.

This document was prepared by Technical Committee ISO/TC 60, *Gears*, Subcommittee SC 2, *Gear capacity calculation*.

This first edition of ISO/TS 6336-21 cancels and replaces ISO/TR 13989-2.

A list of all parts in the ISO 6336 series can be found on the ISO website. See also the Introduction for an overview.

Introduction

The ISO 6336 series consists of International Standards, Technical Specifications (TS) and Technical Reports (TR) under the general title *Calculation of load capacity of spur and helical gears* (see Table 1).

— International Standards contain calculation methods that are based on widely accepted practices and have been validated.

— TS contain calculation methods that are still subject to further development.

— TR contain data that is informative, such as example calculations.

The procedures specified in ISO 6336-1 to ISO 6336-19 cover fatigue analyses for gear rating. The procedures described in ISO 6336-20 to ISO 6336-29 are predominantly related to the tribological behaviour of the lubricated flank surface contact. ISO 6336-30 to ISO 6336-39 include example calculations. The ISO 6336 series allows the addition of new parts under appropriate numbers to reflect knowledge gained in the future.

Requesting standardized calculations according to ISO 6336 without referring to specific parts requires the use of only those parts that are currently designated as International Standards (see Table 1 for listing). When requesting further calculations, the relevant part or parts of ISO 6336 need to be specified. Use of a Technical Specification as acceptance criteria for a specific design needs to be agreed in advance between manufacturer and purchaser.

Table 1 — Overview of ISO 6336

Calculation of load capacity of spur and helical gears	International Standard	Technical Specification	Technical Report
Part 1: Basic principles, introduction and general influence factors	X		
Part 2: Calculation of surface durability (pitting)	X		
Part 3: Calculation of tooth bending strength	X		
Part 4: Calculation of tooth flank fracture load capacity		X	
Part 5: Strength and quality of materials	X		
Part 6: Calculation of service life under variable load	X		
Part 20: Calculation of scuffing load capacity (also applicable to bevel and hypoid gears) — Flash temperature method (Replaces ISO/TR 13989-1)		X	
Part 21: Calculation of scuffing load capacity (also applicable to bevel and hypoid gears) — Integral temperature method (Replaces ISO/TR 13989-2)		X	
Part 22: Calculation of micropitting load capacity (Replaces ISO/TR 15144-1)		X	
Part 30: Calculation examples for the application of ISO 6336-1, ISO 6336-2, ISO 6336-3 and ISO 6336-5			X
Part 31: Calculation examples of micropitting load capacity (Replaces: ISO/TR 15144-2)			X
At the time of publication of this document, some of the parts listed here were under development. Consult the ISO website.			

This document describes the surface damage "warm scuffing" for cylindrical (spur and helical), bevel and hypoid gears for generally used gear materials and different heat treatments. "Warm scuffing" is characterized by typical scuffing and scoring marks, which can lead to increasing power loss, dynamic load, noise and wear. For "cold scuffing", generally associated with low temperature and low speed, under approximately 4 m/s, and through-hardened, heavily loaded gears, the formulae are not suitable.

There is a particularly severe form of gear tooth surface damage in which seizure or welding together of areas of tooth surfaces occurs due to absence or breakdown of a lubricant film between the contacting tooth flanks of mating gears caused by high temperature and high pressure. This form of damage is

termed "scuffing" and most relevant when surface velocities are high. Scuffing may also occur for relatively low sliding velocities when tooth surface pressures are high enough, either generally or, because of uneven surface geometry and loading, in discrete areas.

Risk of scuffing damage varies with the properties of gear materials, the lubricant used, the surface roughness of tooth flanks, the sliding velocities and the load. Excessive aeration or the presence of contaminants in the lubricant such as metal particles in suspension, also increases the risk of scuffing damage. Consequences of the scuffing of high speed gears include a tendency to high levels of dynamic loading due to increase of vibration, which usually leads to further damage by scuffing, pitting or tooth breakage.

High surface temperatures due to high surface pressures and sliding velocities can initiate the breakdown of lubricant films. On the basis of this hypothesis, two approaches to relate temperature to lubricant film breakdown are presented:

— the flash temperature method (presented in ISO/TS 6336-20), based on contact temperatures which vary along the path of contact;

— the integral temperature method (presented in this document), based on the weighted average of the contact temperatures along the path of contact.

The integral temperature method is based on the assumption that scuffing is likely to occur when the mean value of the contact temperature (integral temperature) is equal to or exceeds a corresponding critical value. The risk of scuffing of an actual gear unit can be predicted by comparing the integral temperature with the critical value, derived from a gear test for scuffing resistance of lubricants. The calculation method takes account of all significant influencing parameters, i.e. the lubricant (mineral oil with and without EP-additives, synthetic oils), the surface roughness, the sliding velocities, the load, etc.

In order to ensure that all types of scuffing and comparable forms of surface damage due to the complex relationships between hydrodynamical, thermodynamical and chemical phenomena are dealt with, further methods of assessment may be necessary. The development of such methods is the objective of ongoing research.

Calculation of load capacity of spur and helical gears —

Part 21:
Calculation of scuffing load capacity (also applicable to bevel and hypoid gears) — Integral temperature method

1 Scope

This document specifies the integral temperature method for calculating the scuffing load capacity of cylindrical, bevel and hypoid gears.

2 Normative references

The following documents are referred to in the text in such a way that some or all of their content constitutes requirements of this document. For dated references, only the edition cited applies. For undated references, the latest edition of the referenced document (including any amendments) applies.

ISO 53, *Cylindrical gears for general and heavy engineering — Standard basic rack tooth profile*

ISO 1122-2, *Vocabulary of gear terms — Part 2: Definitions related to worm gear geometry*

ISO 1328-1, *Cylindrical gears — ISO system of flank tolerance classification — Part 1: Definitions and allowable values of deviations relevant to flanks of gear teeth*

ISO 10300-1, *Calculation of load capacity of bevel gears — Part 1: Introduction and general influence factors*

3 Terms, definitions, symbols and units

3.1 Terms and definitions

For the purposes of this document, the terms and definitions given in ISO 1122-2 apply.

ISO and IEC maintain terminological databases for use in standardization at the following addresses:

— ISO Online browsing platform: available at https://www.iso.org/obp

— IEC Electropedia: available at https://www.electropedia.org/

3.2 Symbols and units

The symbols used in this document are given in Table 2.

Table 2 — Symbols and units

Symbol	Description	Unit
a	centre distance	mm
a_v	virtual centre distance of virtual cylindrical gear	mm
b	face width, smaller value of pinion or wheel	mm
b_{eB}	effective facewidth for scuffing	mm
c_v	specific heat capacity per unit volume	N/(mm^2·K)
c'	single stiffness	N/(mm·µm)
c_γ	mesh stiffness	N/(mm·µm)
d	reference circle diameter	mm
d_{Na}	effective tip diameter	mm
d_a	tip diameter	mm
d_b	base diameter	mm
d_m	diameter at mid-facewidth	mm
d_s	reference circle of virtual crossed axes helical gear	mm
d_v	reference diameter of virtual cylindrical gear	mm
d_{va}	tip diameter of virtual cylindrical gear	mm
d_{vb}	base diameter of virtual cylindrical gear	mm
$g_{an1,2}$	recess path of contact of pinion, wheel	mm
$g_{fn1,2}$	approach path of contact of pinion, wheel	mm
g^*	sliding factor	—
h_{am}	addendum at mid-facewidth of hypoid gear	mm
m	module	mm
m_{mn}	normal module of hypoid gear at mid-facewidth	mm
m_{sn}	normal module of virtual crossed axes helical gear	mm
n_p	number of meshing gears	—
p_{en}	normal base pitch	mm
u	gear ratio	—
u_v	gear ratio of virtual cylindrical gear	—
v	reference line velocity	m/s
$v_{tl,2}$	tangential velocity of pinion, wheel of hypoid gear	m/s
v_{gyl}	maximum sliding velocity at tip of pinion	m/s
v_{gs}	sliding velocity at pitch point	m/s
$v_{g1,2}$	sliding velocity	m/s
$v_{g\alpha 1}$	sliding velocity	m/s

Subscripts:

1 pinion

2 wheel

a tip diameter of the virtual gear

b base circle of the virtual gear

m mid-facewidth of bevel or hypoid gears

n normal section

s virtual crossed axes helical gear

t tangential direction

T test gear

Table 2 *(continued)*

Symbol	Description	Unit
$v_{g\beta 1}$	sliding velocity	m/s
v_{mt}	tangential speed at reference cone at mid-facewidth of bevel gear	m/s
$v_{\Sigma C}$	sums of tangential speeds at pitch point	m/s
$v_{\Sigma s}$	tangential speed	m/s
$v_{\Sigma h}$	tangential speed	m/s
w_{Bt}	specific tooth load, scuffing	N/mm
z	number of teeth	—
z_v	number of teeth of virtual cylindrical gear	—
B_M	thermal contact coefficient	N/(mm·s$^{1/2}$·K)
C_1,C_2,C_{2H}	weighting factors	—
C_a	nominal tip relief	µm
C_{eff}	effective tip relief	µm
E	module of elasticity (Young's modulus)	N/mm^2
F_{mt}	nominal tangential load at reference cone at mid-facewidth	N
F_n	normal tooth load	N
F_t	nominal tangential load at reference circle	N
K_A	application factor	—
K_v	dynamic factor	—
$K_{B\alpha}$	= $K_{H\alpha}$ transverse load factor (scuffing)	—
$K_{B\beta}$	= $K_{H\beta}$ face load factor (scuffing)	—
$K_{B\gamma}$	helical load factor (scuffing)	—
$K_{B\beta be}$	bearing factor	—
$K_{H\alpha}$	transverse load factor	—
$K_{H\beta}$	face load factor	—
$K_{H\beta be}$	bearing factor	—
L	contact parameter	—
R_a	arithmetic mean roughness	µm
S_{intS}	scuffing safety factor	—
S_{Smin}	minimum required scuffing safety factor	—
T_1	torque of the pinion	Nm
T_{1T}	scuffing torque of test pinion	Nm
X_{BE}	geometry factor at pinion tooth tip	—
X_E	run-in factor	—
X_{Ca}	tip relief factor	—

Subscripts:

1 pinion
2 wheel
a tip diameter of the virtual gear
b base circle of the virtual gear
m mid-facewidth of bevel or hypoid gears
n normal section
s virtual crossed axes helical gear
t tangential direction
T test gear

Table 2 *(continued)*

Symbol	Description	Unit
X_G	geometry factor of hypoid gears	—
X_L	lubricant factor	—
X_M	thermal flash factor	—
X_Q	approach factor	—
X_R	roughness factor	—
X_S	lubrication factor	—
X_W	welding factor of executed gear	—
X_{WT}	welding factor of test gear	—
X_{WrelT}	relative welding factor	—
X_{mp}	contact factor	—
$X_{\alpha\beta}$	pressure angle factor	—
X_ε	contact ratio factor	—
α	pressure angle	°
α_{mn}	normal pressure angle at mid-facewidth of hypoid gear	°
α_n	normal pressure angle	°
α_{sn}	normal pressure angle of crossed axes helical gear	°
α_{st}	transverse pressure angle of crossed axes helical gear	°
α_t	transverse pressure angle	°
α_t'	transverse working pressure angle	°
α_{vt}	transverse pressure angle of virtual cylindrical gear	°
α_y	arbitrary angle	°
β	helix angle	°
β_b	helix angle at base circle	°
β_m	helix angle at reference cone at mid-facewidth of hypoid gear	°
β_s	helix angle of virtual crossed axes helical gear	°
γ	auxiliary angle	°
δ	reference cone angle	°
ε_a	recess contact ratio	—
ε_f	approach contact ratio	—
ε_n	contact ratio in normal section of virtual crossed axes helical gear	—
ε_1	addendum contact ratio of the pinion	—
ε_2	addendum contact ratio of the wheel	—
ε_α	contact ratio	—
$\varepsilon_{v\alpha}$	transverse contact ratio of virtual cylindrical gear	—

Subscripts:

1 pinion
2 wheel
a tip diameter of the virtual gear
b base circle of the virtual gear
m mid-facewidth of bevel or hypoid gears
n normal section
s virtual crossed axes helical gear
t tangential direction
T test gear

Table 2 *(continued)*

Symbol	Description	Unit
ε_{v1}	tip contact ratio of virtual cylindrical pinion	—
ε_{v2}	tip contact ratio of virtual cylindrical wheel	—
ξ	Hertzian auxiliary coefficient	—
μ_{mC}	mean coefficient of friction	—
η_{oil}	dynamic viscosity at oil temperature	mPa · s
λ_M	heat conductivity	N/(s · K)
ν	Poisson's ratio	—
ν_{40}	kinematic viscosity of the oil at 40 °C	mm^2/s; cSt
$\rho_{E1,2}$	radius of curvature at tip of the pinion, wheel	mm
ρ_{Cn}	relative radius of curvature at pitch point in normal section	mm
$\rho_{n1,2}$	radius of curvature at pitch point in normal section	mm
ρ_{redC}	relative radius of curvature at pitch point	mm
η	Hertzian auxiliary coefficient	—
ϑ	Hertzian auxiliary angle	°
ϑ_{flaE}	flash temperature at pinion tooth tip when load sharing is neglected	K
ϑ_{flaint}	mean flash temperature	K
$\vartheta_{flainth}$	mean flash temperature of hypoid gear	K
ϑ_{int}	integral temperature	K
ϑ_{intP}	permissible integral temperature	K
ϑ_{intS}	scuffing integral temperature (allowable integral temperature)	K
$\vartheta_{flaintT}$	mean flash temperature of the test gear	K
ϑ_{oil}	oil sump or spray temperature	°C
ϑ_{M-C}	bulk temperature	°C
ϑ_{MT}	test bulk temperature	°C
φ	axle angle of virtual crossed axes helical gear	°
Σ	crossing angle of virtual crossed axes helical gear	°
φ_E	run-in grade	—
Γ	parameter on the line of action	—

Subscripts:

1 pinion
2 wheel
a tip diameter of the virtual gear
b base circle of the virtual gear
m mid-facewidth of bevel or hypoid gears
n normal section
s virtual crossed axes helical gear
t tangential direction
T test gear

4 Field of application

4.1 General

The calculation methods are based on results of the rig testing of gears run at pitch line velocities less than 80 m/s. The formulae can be used for gears which run at higher speeds, but with increasing uncertainty as speed increases. The uncertainty concerns the estimation of bulk temperature, coefficient of friction, allowable temperatures, etc. as speeds exceed the range with experimental background.

4.2 Scuffing damage

When once initiated, scuffing damage can lead to gross degradation of tooth flank surfaces, with increase of power loss, dynamic loading, noise and wear. It can also lead to tooth breakage if the severity of the operating conditions is not reduced. In the event of scuffing due to an instantaneous overload, followed immediately by a reduction of load, e.g. by load redistribution, the tooth flanks may self-heal by smoothing themselves to some extent. Even so, the residual damage will continue to be a cause of increased power loss, dynamic loading and noise.

In most cases, the resistance of gears to scuffing can be improved by using a lubricant with enhanced extreme pressure (E.P.) properties. It is important, however, to be aware that some disadvantages attend the use of E.P. oils, e.g corrosion of copper, embrittlement of elastomers, lack of world-wide availability, etc. These disadvantages are to be taken into consideration if optimum lubricant choice is to be made, which means as few additive as possible, as much as necessary.

Due to continuous variation of different parameters, the complexity of the chemical properties and the thermo-hydro-elastic processes in the instantaneous contact area, some scatter in the calculated assessments of probability of scuffing risk, is to be expected.

In contrast to the relatively long time of development of fatigue damage, one single momentary overload can initiate scuffing damage of such severity that affected gears may no longer be used. This should be carefully considered when choosing an adequate safety factor for gears, especially for gears required to operate at high circumferential velocities.

4.3 Integral temperature criterion

This approach to the evaluation of the probability of scuffing, is based on the assumption that scuffing is likely to occur when the mean value of the contact temperatures along the path of contact is equal to or exceeds a corresponding "critical value". In the method presented herein, the sum of the bulk temperature and the weighted mean of the integrated values of flash temperatures along the path of contact is the "integral temperature". The bulk temperature is estimated as described under 6.1.6 and the mean value of the flash temperature is approximated by substituting mean values of the coefficient of friction, the dynamic loading, etc., along the path of contact. A weighting factor is introduced, accounting for possible different influences of a real bulk temperature value and a mathematically integrated mean flash temperature value on the scuffing phenomenon.

The probability of scuffing is assessed by comparing the integral temperature with a corresponding critical value derived from the gear testing of lubricants for scuffing resistance (e.g. different FZG test procedures, the IAE and the Ryder gear tests) or from gears which have scuffed in service.

5 Influence factors

5.1 Mean coefficient of friction, μ_{mC}

The actual coefficient of friction between the tooth flanks is an instantaneous and local value which depends on several properties of the oil, surface roughness, lay of the surface irregularities such as those left by machining, properties of the tooth flank materials, tangential velocities, forces at the

surfaces and the dimensions. Assessment of the instantaneous coefficient of friction is difficult since there is no method currently available for its measurement.

The mean value for the coefficient of friction, μ_{mC}, along the path of contact was derived from measurements[4] and approximated by Formula (1). Although the local coefficient of friction is near to zero in the pitch point C, the mean value can be approximated with the parameters at the pitch point and the oil viscosity, η_{oil}, at oil temperature, ϑ_{oil}, when introduced into Formula (1).

$$\mu_{mC} = 0{,}045 \cdot \left(\frac{w_{Bt} \cdot K_{B\gamma}}{v_{\Sigma C} \cdot \rho_{redC}} \right)^{0,2} \cdot \eta_{oil}^{-0,05} \cdot X_R \cdot X_L \quad (1)$$

Note Formula (1) is derived from testing of gears with centre distance $a \approx 100$ mm.

The coefficient of friction of the integral temperature method takes account of the size of the gear in a different way as the coefficient of friction of the flash temperature method. Formula (1) for calculating the coefficient of friction should not be applied outside the field of the part where it is presented, e.g. coefficient of friction for thermal rating.

$$\mu_{mc} = 0{,}048 \cdot \left(\frac{F_{bt} / b}{v_{\Sigma C} \cdot \rho_{redC}} \right)^{0,2} \cdot \eta_{oil}^{-0,05} \cdot R_a^{0,25} \cdot X_L \quad (2)$$

where

X_L is $0{,}75 \cdot \left(\frac{6}{v_{\Sigma C}}\right)^{0,2}$ 1 for polyglycols;

X_L is 1,0 for mineral oils;

X_L is 0,8 for polyalfaolefins;

X_L is 1,5 for traction fluids;

X_L is 1,3 for phosphate esters.

Formula (2) represents results of tests within a range of a = 91,5 mm to 200 mm. The application of this formula makes it necessary to adjust Figures 9, 10 and 11 for the scuffing temperature, ϑ_{intS}, accordingly.

The formula for the calculation of μ_{mC} was derived from experiments in the following range of operating conditions. Extrapolation may lead to deviations between the calculated and the real coefficient of friction.

$1 \text{ m/s} \leq v \leq 50 \text{ m/s}$

At reference line velocities, v, lower than 1 m/s, higher coefficients of friction are expected. At reference line velocities, v, higher than 50 m/s, the limiting value of $v_{\Sigma C}$ at v = 50 m/s has to be used in Formula (1).

$w_{Bt} \geq 150 \text{ N/mm}$

For lower values of the specific normal tooth load, w_{Bt}, the limiting value, w_{Bt} = 150 N/mm, has to be used in Formula (1).

$$v_{\Sigma C} = 2 \cdot v \cdot \tan \alpha_{t'} \cdot \cos \alpha_t \tag{3}$$

$$\rho_{redC} = \frac{u}{(1+u)^2} \cdot a \cdot \frac{\sin \alpha_{t'}}{\cos \beta_b} \tag{4}$$

$$w_{Bt} = K_A \cdot K_v \cdot K_{B\beta} \cdot K_{B\alpha} \cdot \frac{F_t}{b} \tag{5}$$

$K_{B\gamma}$ is the helical load factor. Scuffing takes account of increasing friction for increasing total contact ratio (see Figure 1).

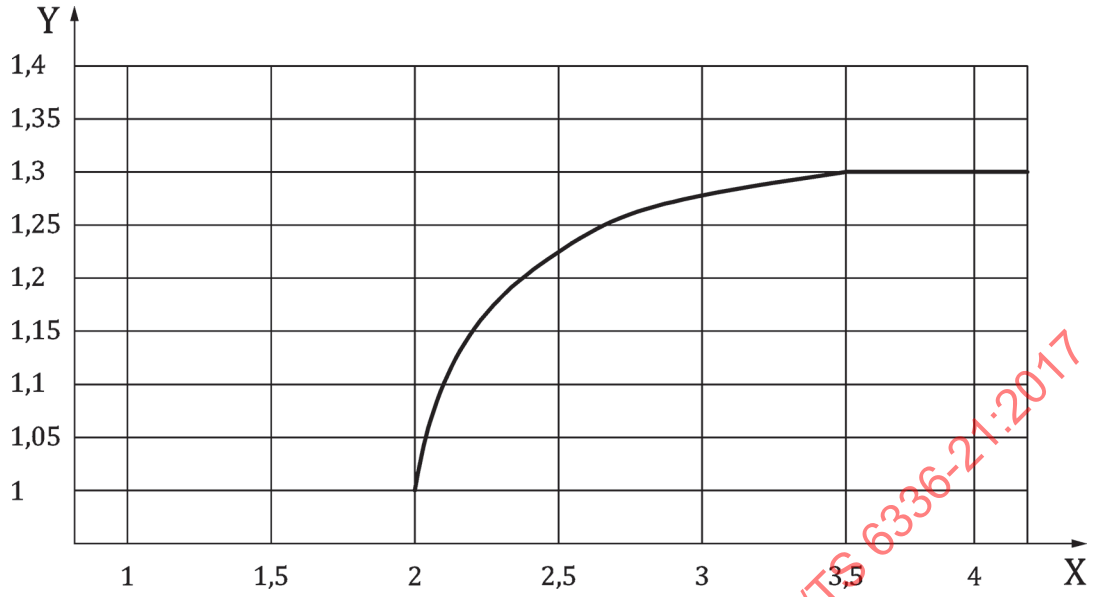

Key

X total contact ratio, ε_γ

Y helical load factor, $K_{B\gamma}$

Figure 1 — Helical load factor, $K_{B\gamma}$

$$K_{B\gamma} = \begin{cases} 1 & \text{for } \varepsilon_\gamma \leq 2 \\ 1 + 0{,}2 \cdot \sqrt{(\varepsilon_\gamma - 2) \cdot (5 - \varepsilon_\gamma)} & \text{for } 2 < \varepsilon_\gamma < 3{,}5 \\ 1{,}3 & \text{for } \varepsilon_\gamma \geq 3{,}5 \end{cases} \quad (6)$$

$$R_a = 0{,}5 \cdot (R_{a1} + R_{a2}) \quad (7)$$

R_{a1} and R_{a2} are the tooth flank roughness values of pinion and wheel measured on the new flanks as manufactured (e.g. reference test gear roughness values, R_a, are ≈ 0,35 µm).

$$X_R = 2{,}2 \cdot (R_a / \rho_{redC})^{0{,}25} \quad (8)$$

where

X_L is 1,0 for mineral oils;

X_L is 0,8 for polyalfaolefins;

X_L is 0,7 for non-water-soluble polyglycols;

X_L is 0,6 for water-soluble polyglycols;

X_L is 1,5 for traction fluids;

X_L is 1,3 for phosphate esters.

5.2 Run-in factor, X_E

The present calculation methods presume that the gears are well run-in. In practice, scuffing failure occurs very often during the first few hours in service, e.g. in a full load test run, the acceptance run of vessels or when a new set of gears is built into a production machinery when the gears are run under

full load conditions before a proper run-in. Investigations[4] show a 1/4 to 1/3 load carrying capacity of a newly manufactured gear flank compared to a properly run-in flank. This should be taken into account by a run-in factor, X_E, as shown in Formula 9:

$$X_E = 1 + (1 - \varphi_E) \cdot \frac{30 \cdot R_a}{\rho_{redC}} \tag{9}$$

where

φ_E is 1, full run-in (for carburized and ground gears full run-in can be assumed if $R_{a\ run\text{-}in} \approx 0{,}6\ R_{a\ new}$);

φ_E is 0, newly manufactured.

5.3 Thermal flash factor, X_M

The thermal flash factor, X_M, accounts for the influence of the properties of the pinion and gear materials on the flash temperature.

Calculation of the thermal flash factor for an arbitrary point (index y) on the line of action (see Figure 2) is shown in Formula (10):

$$X_M = \left(\frac{2}{\frac{1-ny_1^2}{E_1} + \frac{1-ny_2^2}{E_2}} \right)^{0,25} \cdot \frac{\sqrt{(1+\Gamma)} + \sqrt{(1-\frac{\Gamma}{u})}}{B_{M1} \cdot \sqrt{(1+\Gamma)} + B_{M2} \cdot \sqrt{(1-\frac{\Gamma}{u})}} \tag{10}$$

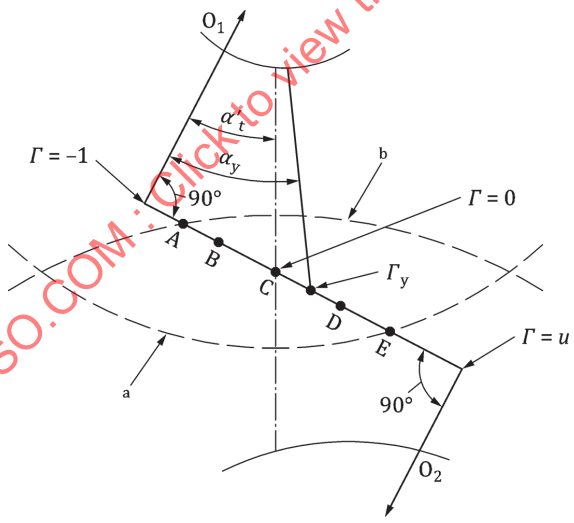

a Tip circle 1.

b Tip circle 2.

Figure 2 — Parameter Γ on the line of action

$$\Gamma = \frac{\tan\alpha_y}{\tan\alpha_{t'}} - 1 \tag{11}$$

If the materials of pinion and wheel are the same, Formula (10) can be simplified as shown in Formula (12):

$$X_M = \frac{E^{0,25}}{(1-ny^2)^{0,25} \cdot B_M} \tag{12}$$

In the above formula, the thermal contact coefficient, B_M, is shown in Formula (13):

$$B_M = \sqrt{(\lambda_M \cdot c_v)} \tag{13}$$

For case hardened steels with the following typical characteristic values:

λ_M = 50 N/(s · K), c_v = 3,8 N/(mm² · K), E = 206 000 N/mm² and v = 0,3

follows

X_M = 50,0 K · N$^{-0,75}$ · s^{0,5} · m$^{-0,5}$ · mm

For the characteristic values of other materials, see Reference [10].

5.4 Pressure angle factor, $X_{\alpha\beta}$

The pressure angle factor, $X_{\alpha\beta}$, is used to account for the conversion of load and tangential speed from reference circle to pitch circle.

Method A: Factor $X_{\alpha\beta\text{-A}}$ is shown in Formula (14):

$$X_{\alpha\beta\text{-A}} = 1,22 \cdot \frac{(\sin^{0,25}\alpha_{t'} \cdot \cos^{0,25}\alpha_n \cdot \cos^{0,25}\beta)}{(\cos^{0,5}\alpha_{t'} \cdot \cos^{0,5}\alpha_t)} \tag{14}$$

Table 3 shows the values for the pressure angle factor, $X_{\alpha\beta}$, for a standard rack with pressure angle, α_n = 20°, the typical range of standard working pressure angles, α_t', and helix angles, β.

Table 3 — Method B: Factor $X_{\alpha\beta\text{-B}}$

α_t'	β = 0°	10°	20°	30°
19°	0,963	0,960	0,951	0,938
20°	0,978	0,975	0,966	0,952
21°	0,992	0,989	0,981	0,966
22°	1,007	1,004	0,995	0,981
23°	1,021	1,018	1,009	0,995
24°	1,035	1,032	1,023	1,008
25°	1,049	1,046	1,037	1,012

As an approximation, for gears with normal pressure angle, α_n = 20°, the pressure angle factor can be approximated as follows:

$X_{\alpha\beta\text{-B}}$ = 1

6 Calculation

6.1 Cylindrical gears

6.1.1 General

This clause contains formulae which enable the assessment of the "probability of scuffing" (warm scuffing) of oil-lubricated, involute spur and helical gears.

It is assumed that the total tangential load is equally distributed between the two helices of double helical gears. When, due to application of forces such as external axial forces, this is not the case, the influences of these are to be taken into account separately. The two helices are to be treated as parallel single helical gears. Influences affecting scuffing probability, for which quantitative assessments can be made, are included.

The formulae are valid for gears with external or internal teeth which are conjugate to a basic rack as defined in ISO 53. For internal gears, negative values have to be introduced for the determination of the geometry factor, X_{BE}, as presented in 6.1.11. They may also be considered as valid for similar gears of other basic rack forms, of which the transverse contact ratio is $\varepsilon_\alpha \leq 2{,}5$.

6.1.2 Scuffing safety factor, S_{intS}

As uncertainties and inaccuracies in the assumptions cannot be excluded, it is necessary to introduce a safety factor, S_{intS}. It must be pointed out, that the scuffing safety factor is temperature-related and is not a factor by which gear torque may be multiplied to arrive at the same values for the integral temperature number, ϑ_{int}, and the scuffing integral temperature number, ϑ_{intS}.

$$S_{intS} = \frac{\vartheta_{intS}}{\vartheta_{int}} \geq S_{Smin} \tag{15}$$

Recommendation for choosing S_{Smin}:

$S_{Smin} < 1$ High scuffing risk

$1 \leq S_{Smin} \leq 2$ Critical range with moderate scuffing risk, influenced by the operating conditions of the actual gear. Influencing factors are, e.g. the tooth flank roughness, run-in effects, the accurate knowledge of the load factors, the load capacity of lubricating oil, etc.

$S_{Smin} > 2$ Low scuffing risk

Given the relationship between the actual load and the integral temperature number, the corresponding load safety factor, S_{Sl}, can be approximated by Formula (16):

$$S_{Sl} = \frac{w_{Btmax}}{w_{Bteff}} \approx \frac{\vartheta_{intS} - \vartheta_{oil}}{\vartheta_{int} - \vartheta_{oil}} \tag{16}$$

6.1.3 Permissible integral temperature, ϑ_{intP}

$$\vartheta_{intP} = \frac{\vartheta_{intS}}{S_{Smin}} \tag{17}$$

The minimum required scuffing safety factor, S_{Smin}, is to be separately determined for each application.

6.1.4 Integral temperature, ϑ_{int}

$$\vartheta_{int} = \vartheta_M + C_2 \cdot \vartheta_{flaint} \leq \vartheta_{intP} \tag{18}$$

where C_2 is the weighting factor derived from experiments. For spur and helical gears, C_2 = 1,5.

$$\vartheta_{flaint} = \vartheta_{flaE} \cdot X_\varepsilon \tag{19}$$

6.1.5 Flash temperature at pinion tooth tip, ϑ_{flaE}

The flash temperature is the calculated increase in gear tooth surface temperature at a given point along the path of contact resulting from the combined effects of gear tooth geometry, load, friction, velocity and material properties during operation.

$$\vartheta_{flaE} = \mu_{mC} \cdot X_M \cdot X_{BE} \cdot X_{\alpha\beta} \cdot \frac{(K_{B\gamma} \cdot w_{Bt})^{0,75} \cdot v^{0,5}}{|a|^{0,25}} \cdot \frac{X_E}{X_Q \cdot X_{Ca}} \tag{20}$$

6.1.6 Bulk temperature, ϑ_M

6.1.6.1 General

The bulk temperature is the temperature of the tooth surfaces immediately before they come into contact.

The bulk temperature is established by the thermal balance of the gear unit. There are several sources of heat in a gear unit of which the most important are tooth and bearing friction. Other sources of heat, such as seals and oil flow, contribute to some extent. At pitch line velocities in excess of 80 m/s, heat from the churning of oil in the mesh and windage losses may become significant and should be taken into consideration (see Method A). The heat is transferred to the environment via the housing walls by conduction, convection and radiation and for spray lubrication conditions through the oil into an external heat exchanger.

Values obtained using the different calculation methods described below are to be distinguished by the subscripts A, B and C.

6.1.6.2 Method A, $\vartheta_{M\text{-}A}$

The bulk temperature as a mean value or as temperature distribution over the facewidth can be measured experimentally or be determined by a theoretical analysis based on known power loss and heat transfer data, i.e. by using thermal network methods.

6.1.6.3 Method B, $\vartheta_{M\text{-}B}$

This method is not used for the integral temperature method (see the flash temperature method given in ISO/TS 6336-20).

6.1.6.4 Method C, $\vartheta_{M\text{-}C}$

An approximate value for the bulk temperature consists of the sum of the oil temperature and a part of a mean value derived from the flash temperature over the path of contact according to method C, as shown in Formula (21):

$$\vartheta_{M\text{-}C} = \vartheta_{oil} + C_1 \cdot X_{mp} \cdot \vartheta_{flaint} \cdot X_S \tag{21}$$

where

X_S is 1,2 for spray lubrication;

X_S is 1,0 for dip lubrication;

X_S is 0,2 for gears submerged in oil;

C_1 is the constant accounting for heat transfer conditions, from test results C_1 = 0,7.

$$X_{mp} = \frac{1 + n_p}{2} \tag{22}$$

where n_p is the number of meshing gears.

6.1.7 Mean coefficient of friction, μ_{mC}

See 5.1.

6.1.8 Run-in factor, X_E

See 5.2.

6.1.9 Thermal flash factor, X_M

See 5.3.

6.1.10 Pressure angle factor, $X_{\alpha\beta}$

See 5.4.

6.1.11 Geometry factor at tip of pinion, X_{BE}

The geometry factor, X_{BE}, takes account for Hertzian stress and sliding velocity at the pinion tooth tip. X_{BE} is a function of the gear ratio, u, and the radius of curvature, ρ_E, at the pinion tooth tip, E.

For internal gears, the following parameters have to be introduced as negative values:

— number of teeth, z_2;

— gear ratio, u;

— centre distance, a;

— all diameters.

$$X_{BE} = 0{,}51 \cdot \sqrt{\frac{|z_2|}{z_2} \cdot (u + 1)} \cdot \frac{\sqrt{\rho_{E1}} - \sqrt{\frac{\rho_{E2}}{u}}}{(\rho_{E1} \cdot |\rho_{E2}|)^{0{,}25}} \tag{23}$$

$$\rho_{E1} = 0{,}5 \cdot \sqrt{d_{a1}^2 - d_{b1}^2} \tag{24}$$

$$\rho_{E2} = a \cdot \sin\alpha_{t'} - \rho_{E1} \tag{25}$$

6.1.12 Approach factor, X_Q

The approach factor, X_Q, takes into account impact loads at the ingoing mesh (at the tooth tip of driven gear) in areas of high sliding. It is represented by a function of the quotient of the approach contact ratio, ε_f, over the recess contact ratio, ε_a (see Figure 3).

$$X_Q = 1{,}00 \qquad \text{for} \quad \frac{\varepsilon_f}{\varepsilon_a} \leq 1{,}5 \tag{26}$$

$$X_Q = 1{,}40 - \frac{4}{15} \cdot \frac{\varepsilon_f}{\varepsilon_a} \qquad \text{for} \quad 1{,}5 < \frac{\varepsilon_f}{\varepsilon_a} < 3 \tag{27}$$

$$X_Q = 0{,}60 \qquad \text{for} \quad 3 \leq \frac{\varepsilon_f}{\varepsilon_a} \tag{28}$$

$$\left.\begin{aligned} \varepsilon_f &= \varepsilon_2 \\ \varepsilon_a &= \varepsilon_1 \end{aligned}\right\} \quad \text{when the pinion drives the wheel} \tag{29}$$

$$\left.\begin{aligned} \varepsilon_f &= \varepsilon_1 \\ \varepsilon_a &= \varepsilon_2 \end{aligned}\right\} \quad \text{when the pinion is driven by the wheel} \tag{30}$$

$$\varepsilon_1 = \frac{z_1}{2\pi} \cdot \left[\sqrt{\left(\frac{d_{a1}}{d_{b1}} \right)^2 - 1} - \tan \alpha_{t'} \right] \tag{31}$$

$$\varepsilon_2 = \frac{|z_2|}{2\pi} \cdot \left[\sqrt{\left(\frac{d_{a2}}{d_{b2}} \right)^2 - 1} - \tan \alpha_{t'} \right] \tag{32}$$

When tooth tips are chamfered or rounded, the tip diameter, d_a, has to be substituted by the effective tip diameter, d_{Na}, at which the recess is starting.

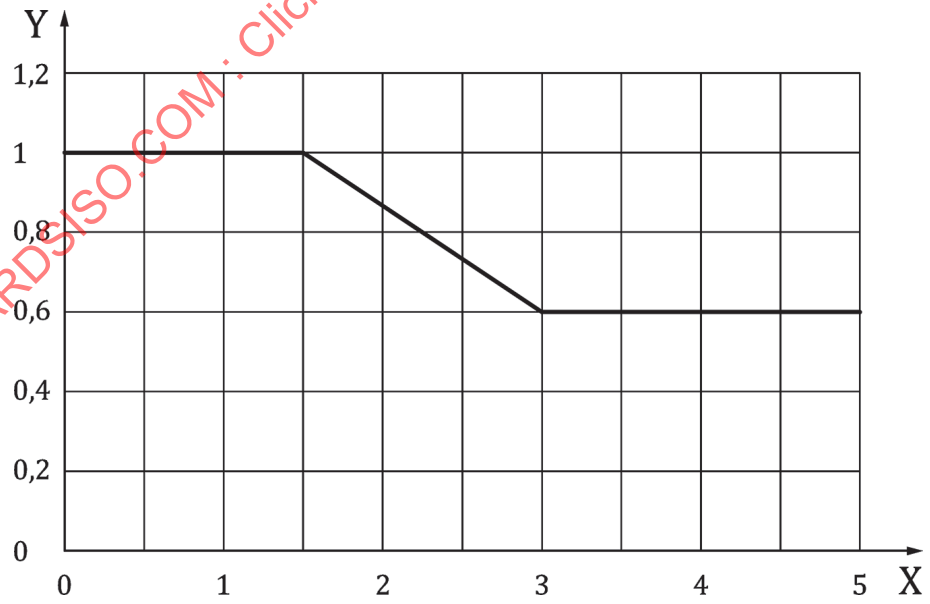

Key

X approach contact ratio, ε_f/recess contact ratio, ε_a

Y approach factor, X_Q

Figure 3 — Approach factor, X_Q

6.1.13 Tip relief factor, X_{Ca}

Elastic deformations of loaded teeth may cause high impact loads at tooth tips in areas of relatively high sliding. The tip relief factor, X_{Ca}, takes account of the influences of profile modifications on such loads. X_{Ca} is a relative tip relief factor which depends on the actual amount of tip relief, C_a, related to the effective tip relief due to elastic deformation, C_{eff} (see Figure 4).

The curves in Figure 4 can be approximated by Formula 32:

$$X_{Ca} = 1 + \left[0{,}06 + 0{,}18\left(\frac{C_a}{C_{eff}}\right)\right] \cdot \varepsilon_{max} + \left[0{,}02 + 0{,}69\left(\frac{C_a}{C_{eff}}\right)\right] \cdot \varepsilon_{max}^{\,2} \quad (33)$$

where ε_{max} is the maximum value, ε_1 or ε_2.

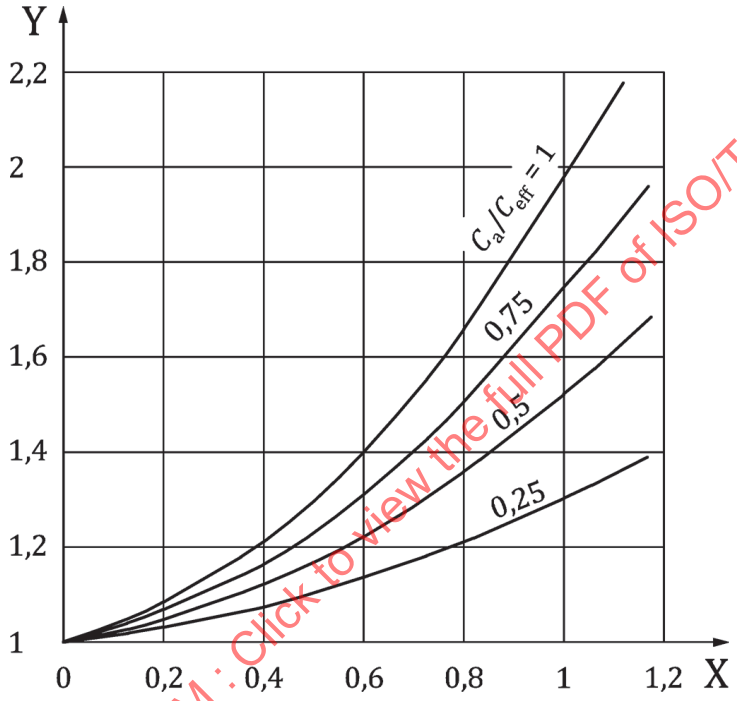

Key

X maximum value, ε_{max}, of ε_1 or ε_2

Y tip relief factor, X_{ca}

Figure 4 — Tip relief factor, X_{Ca}, due to experimental data[11][12]

The nominal amount of tip relief, C_a, to be introduced into Formula (33) depends on the actual values of tip relief, C_a and, C_{a2}, the effective tip relief, C_{eff}, the ratio of addendum contact ratios and the direction of power flow.

When the pinion drives the wheel and $\varepsilon_1 > 1{,}5\ \varepsilon_2$ or the pinion is driven by the wheel and $\varepsilon_1 > (2/3)\ \varepsilon_2$,

$$C_a = C_{a1} \quad \text{for} \quad C_{a1} \le C_{eff} \quad (34)$$

$$C_a = C_{eff} \quad \text{for} \quad C_{a1} > C_{eff} \quad (35)$$

When the pinion drives the wheel and $\varepsilon_1 \le 1{,}5\ \varepsilon_2$ or the pinion is driven by the wheel and $\varepsilon_1 < (2/3)\ \varepsilon_2$,

$$C_a = C_{a2} \quad \text{for} \quad C_{a2} \le C_{eff} \quad (36)$$

$$C_a = C_{eff} \quad \text{for} \quad C_{a2} > C_{eff} \tag{37}$$

where C_{eff} is the effective tip relief, that amount of tip relief which compensates for the elastic deformation of the teeth in single pair contact.

$$C_{eff} + \frac{K_A \cdot F_t}{b \cdot c'} \text{ for spur gears} \tag{38}$$

$$C_{eff} + \frac{K_A \cdot F_t}{b \cdot c_\gamma} \text{ for helical gears} \tag{39}$$

where b is the facewidth.

If the facewidth of the pinion is different from that of the wheel, the smaller is determinant.

Tip relief, as described above, applies to gears of ISO accuracy grade 6 or better, in accordance with ISO 1328-1. For less accurate gears, X_{Ca} is to be set equal to 1 (see also ISO 6336-1).

6.1.14 Contact ratio factor, X_ε

The contact ratio factor, X_ε, converts the flash temperature value at the pinion tooth tip, when load sharing is neglected, to a mean value of the flash temperature over the path of contact. The contact ratio factor can be expressed in terms of addendum contact ratios, ε_1 and ε_2, and their sum ε_α. The formulae for X_ε are based on an assumed linearity of the flash temperature over the path of contact. Possible errors due to this approach will be unlikely to exceed 5 % and will always be on the safe side.

For $\varepsilon_\alpha < 1$, $\varepsilon_1 < 1$, $\varepsilon_2 < 1$:

$$X_\varepsilon + \frac{1}{2 \cdot \varepsilon_\alpha \cdot \varepsilon_1} \cdot \left({\varepsilon_1}^2 + {\varepsilon_2}^2 \right) \tag{40}$$

For $1 \le \varepsilon_\alpha < 2$, $\varepsilon_1 < 1$, $\varepsilon_2 < 1$ (see Figure 5):

$$X_\varepsilon = \frac{1}{2 \cdot \varepsilon_\alpha \cdot \varepsilon_1} \cdot \left[0{,}70 \cdot \left({\varepsilon_1}^2 + {\varepsilon_2}^2 \right) - 0{,}22 \cdot \varepsilon_\alpha + 0{,}52 - 0{,}60 \cdot \varepsilon_1 \cdot \varepsilon_2 \right] \tag{41}$$

For $1 \le \varepsilon_\alpha < 2$, $\varepsilon_1 \ge 1$, $\varepsilon_2 < 1$:

$$X_\varepsilon = \frac{1}{2 \cdot \varepsilon_\alpha \cdot \varepsilon_1} \cdot \left(0{,}18 \cdot {\varepsilon_1}^2 + 0{,}70 \cdot {\varepsilon_2}^2 + 0{,}82 \cdot \varepsilon_1 - 0{,}52 \cdot \varepsilon_2 - 0{,}30 \cdot \varepsilon_1 \cdot \varepsilon_2 \right) \tag{42}$$

For $1 \le \varepsilon_\alpha < 2$, $\varepsilon_1 < 1$, $\varepsilon_2 \ge 1$:

$$X_\varepsilon = \frac{1}{2 \cdot \varepsilon_\alpha \cdot \varepsilon_1} \cdot \left(0{,}70 \cdot {\varepsilon_1}^2 + 0{,}18 \cdot {\varepsilon_2}^2 - 0{,}52 \cdot \varepsilon_1 + 0{,}82 \cdot \varepsilon_2 - 0{,}30 \cdot \varepsilon_1 \cdot \varepsilon_2 \right) \tag{43}$$

For $2 \le \varepsilon_\alpha < 3$, $\varepsilon_1 \ge \varepsilon_2$ (see Figure 6):

$$X_\varepsilon = \frac{1}{2 \cdot \varepsilon_\alpha \cdot \varepsilon_1} \cdot \left(0{,}44 \cdot {\varepsilon_1}^2 + 0{,}59 \cdot {\varepsilon_2}^2 + 0{,}30 \cdot \varepsilon_1 - 0{,}30 \cdot \varepsilon_2 - 0{,}15 \cdot \varepsilon_1 \cdot \varepsilon_2 \right) \tag{44}$$

For $2 \le \varepsilon_\alpha < 3$, $\varepsilon_1 < \varepsilon_2$ (see Figure 6):

$$X_\varepsilon = \frac{1}{2 \cdot \varepsilon_\alpha \cdot \varepsilon_1} \cdot \left(0{,}59 \cdot {\varepsilon_1}^2 + 0{,}44 \cdot {\varepsilon_2}^2 - 0{,}30 \cdot \varepsilon_1 + 0{,}30 \cdot \varepsilon_2 - 0{,}15 \cdot \varepsilon_1 \cdot \varepsilon_2 \right) \tag{45}$$

$$\varepsilon_\alpha = \varepsilon_1 + \varepsilon_2 \tag{46}$$

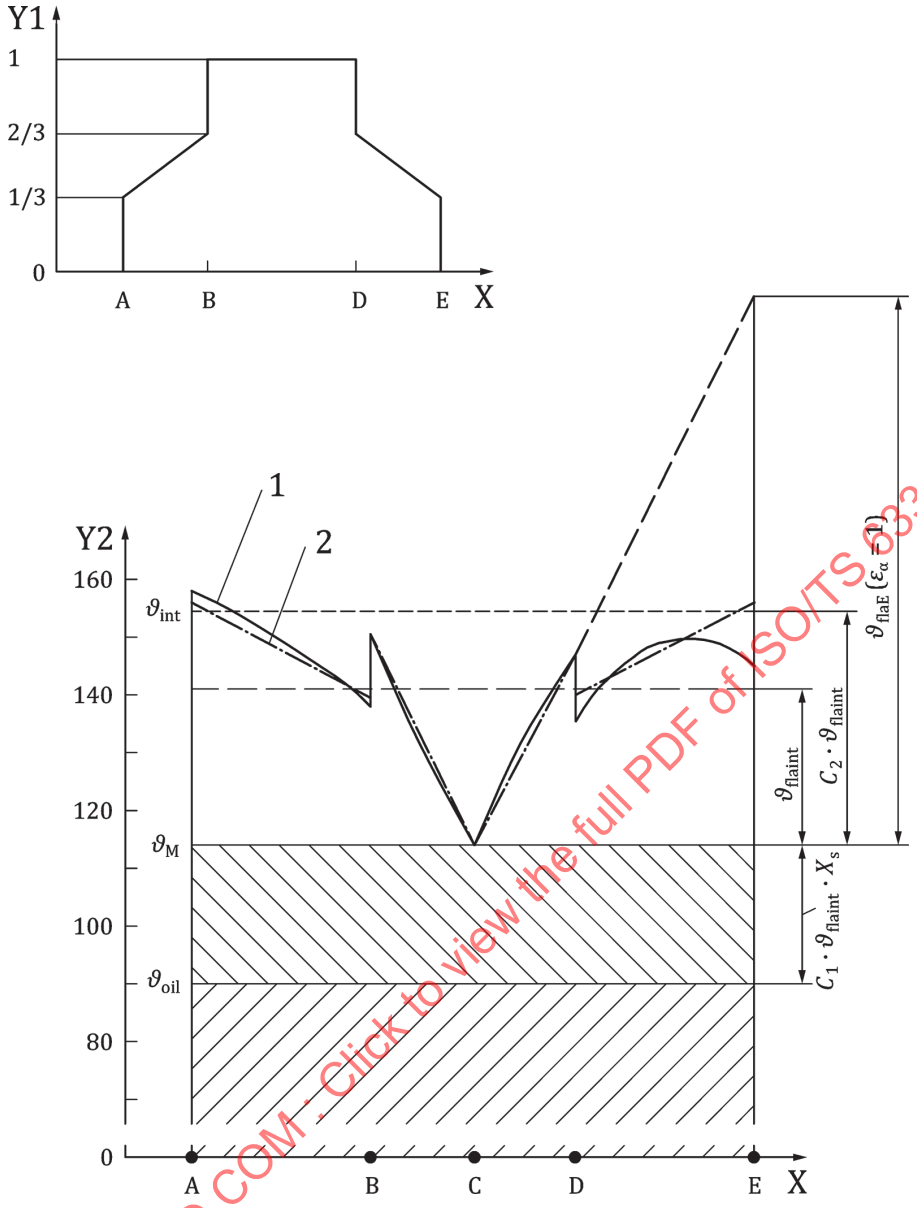

Key

1 distribution of contact temperature
2 approximated distribution
X path of contact
Y1 load
Y2 temperature, °C

Figure 5 — Load and temperature distribution for $1{,}0 \leq \varepsilon_\alpha < 2{,}0$

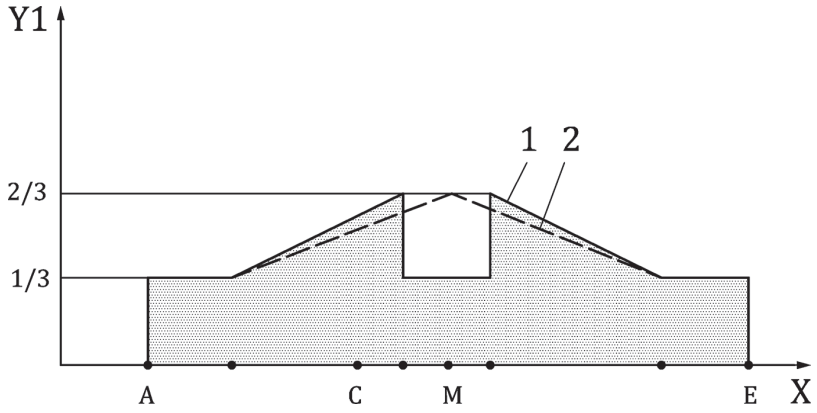

a) Load distribution along the path of contact

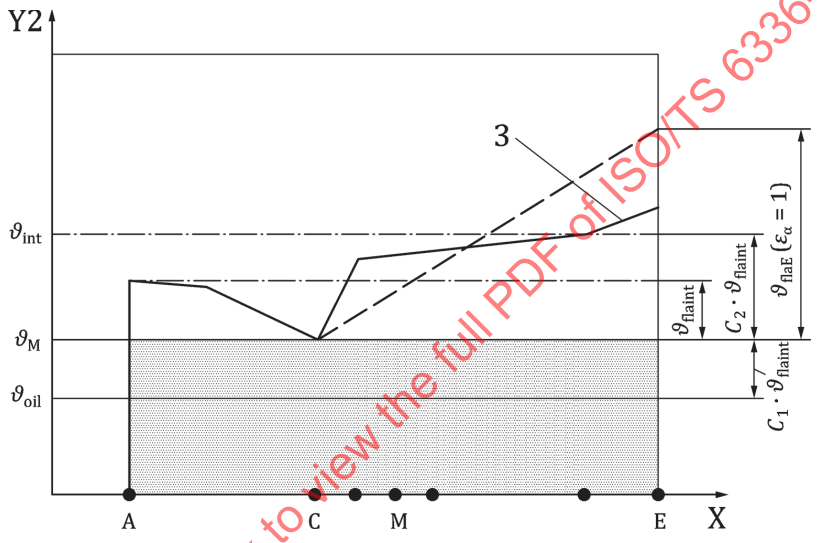

b) Temperature distribution along the path of contact

Key

1 real load distribution
2 approximated load distribution
3 distribution of contact temperature
X path of contact
Y1 load
Y2 temperature

Figure 6 — Load and temperature distribution for $2{,}0 \leq \varepsilon_\alpha < 3{,}0$

6.2 Bevel gears

6.2.1 General

This document follows the integral temperature method as described in 6.1.

For the calculation, the bevel gears are approximated by equivalent cylindrical gears at the mean diameter, d_m, of the bevel gear set (see ISO 10300-1 for the calculation of the virtual cylindrical gear). For this reason, the structure of the calculation methods specified in this document corresponds to that of cylindrical gears.

Scuffing is calculated according to 6.1.1 for the virtual cylindrical gear substituting the bevel gear at the mean diameter in the transverse section.

6.2.2 Scuffing safety factor, S_{intS}

See 6.1.2.

6.2.3 Permissible integral temperature , ϑ_{intP}

See 6.1.3.

6.2.4 Permissible integral temperature, ϑ_{intP}

See 6.1.3.

C_2 = 1,5 for virtual cylindrical gear

6.2.5 Flash temperature at pinion tooth tip, ϑ_{flaE}

See 6.1.5, with the following substitutions:

— in Formula (20): a_v instead of a

v_{mt} instead of v

— in Formula (5): F_{mt} instead of F_t

b_{eB} instead of b

The effective face width, b_{eB}, takes account of the crowning of bevel gears.

$$b_{eB} = 0{,}85 \cdot b_2 \tag{47}$$

where b_2 is the common tooth width of pinion and wheel.

The factors K_A, K_v, $K_{B\beta} = K_{H\beta}$ and $K_{B\alpha} = K_{H\alpha}$ shall be determined in accordance with ISO 10300-1.

$K_{B\gamma}$ = 1

6.2.6 Bulk temperature, ϑ_M

See 6.1.6.

6.2.7 Mean coefficient of friction, μ_{mC}

See 5.1, with the following substitutions:

— in Formula (5): F_{mt} instead of F_t

b_{eB} instead of b

For the conditions of usual bevel gear design, $\alpha_t' = \alpha_{vt}$, i.e. $x_1 = -x_2$:

$$v_{\Sigma C} = 2 \cdot v_{mt} \cdot \sin\alpha_{vt} \tag{48}$$

$K_{B\gamma}$ = 1

6.2.8 Run-in factor, X_E

See 5.2.

6.2.9 Thermal flash factor, X_M

See 5.3.

6.2.10 Pressure angle factor, $X_{\alpha\beta}$

6.2.10.1 Method A: Factor $X_{\alpha\beta\text{-A}}$

For the conditions of usual bevel gear design, $\alpha_t' = \alpha_{vt}$, i.e. $x_1 = -x_2$:

$$X_{\alpha\beta\text{-A}} = 1{,}22 \cdot \frac{\sin^{0,25}\alpha_n}{\cos^{0,75}\alpha_{vt}} \tag{49}$$

6.2.10.2 Method B: Factor $X_{\alpha\beta\text{-B}}$

See 5.4.

6.2.11 Geometry factor at tip of pinion, X_{BE}

See 6.1.11, with the following substitutions:

— in Formula (23): u_v instead of u

— in Formula (24): d_{va1} instead of d_{a1}

d_{vb1} instead of d_{b1}

— in Formula (25): α_{vt} instead of α_t'

6.2.12 Approach factor, X_Q

See 6.1.12, with the following substitutions:

— in Formula (29) to (32): ε_{v1} instead of ε_1

ε_{v2} instead of ε_2

— in Formula (31) and (32): $d_{va1,2}$ instead of $d_{a1,2}$

$d_{vb1,2}$ instead of $d_{b1,2}$

α_{vt} instead of α_t'

$z_{v1,2}$ instead of $z_{1,2}$

6.2.13 Tip relief factor, X_{Ca}

See 6.1.13, with the following substitution:

— in Formula (33): ε_{vmax} instead of ε_{max}

ε_{vmax} maximum value ε_{v1} or ε_{v2}

It is assumed that tip and root relief are chosen as optimum values for the operation conditions (full-load contact pattern spreads just to tip without concentration). Then the following approximation applies:

$$C_a = C_{eff} \text{ and } \frac{C_a}{C_{eff}} = 1 \tag{50}$$

6.2.14 Contact ratio factor, X_ε

See 6.1.14, with the following substitutions in Formulae (39) to (45) and its conditions of validity:

— $\varepsilon_{v\alpha}$ instead of ε_α;

— ε_{v1} instead of ε_1;

— ε_{v2} instead of ε_2.

6.3 Hypoid gears

6.3.1 General

This calculation method of the scuffing resistance of hypoid gears follows the integral temperature criterion of cylindrical gears according to 6.1.

For the calculation of the scuffing resistance, the hypoid gears are approximated by equivalent crossed axes helical gears with the same sliding conditions as the actual hypoid gears (see 6.3.12 for the virtual crossed axes helical gear pair).

6.3.2 Scuffing safety factor, S_{intS}

See 6.1.2.

6.3.3 Permissible integral temperature, ϑ_{intP}

See 6.1.3.

6.3.4 Integral temperature, ϑ_{nt}

See 6.1.4, with the following substitutions:

— in Formula (18): C_{2H} instead of C_2 (C_{2H} = 1,8 according to test results)

$\vartheta_{flainth}$ instead of ϑ_{flaint}

$$\vartheta_{flainth} = 110 \cdot \sqrt{F_n \cdot K_A \cdot K_{B\beta} \cdot v_{t1} \cdot \mu_{mC}} \cdot \frac{X_E \cdot X_G \cdot X_\varepsilon}{X_Q \cdot X_{CA}} \quad (51)$$

$$F_n = \frac{2\,000 \cdot T_1}{\cos\alpha_{mn} \cdot \cos\beta_{m1} \cdot d_{m1}} \quad (52)$$

$$K_{B\beta} = 1{,}5 \cdot K_{B\beta be} \quad (53)$$

$K_{B\beta be} = K_{H\beta be}$ (see ISO 10300-1).

6.3.5 Bulk temperature, ϑ_M

See 6.1.6.

6.3.6 Mean coefficient of friction, μ_{mC}

See 5.1, with the following substitutions:

— in Formula (1): ρ_{Cn} instead of $\rho_{red\,C}$

— in Formula (5): $b_{eB}/\cos\beta_{b2}$ instead of b

F_n instead of F_t

b_{eB}: see Formula (47).

$K_{B\gamma} = 1$

$$K_{B\beta} \cdot K_{B\alpha} = 2{,}0 \text{ (approximation only for the calculation of } \mu_{mc}) \tag{54}$$

X_R [see Formula (8)] with ρ_{Cn} instead of ρ_{redC}.

6.3.7 Run-in factor, X_E

See 5.2, with the following substitution in Formula (9):

— ρ_{Cn} instead of ρ_{redC}

6.3.8 Geometry factor, X_G

The geometry factor, X_G, accounts for the mean Hertzian stress and the mean contact length along the path of contact. As an approximation it can be determined by using the values at the pitch point (ρ_{Cn}, L).

$$X_G = \frac{\frac{\sin\Sigma}{\cos\beta_{s2}} \cdot \sqrt{\frac{1}{\rho_{Cn}}}}{\sqrt{L \cdot \sin\beta_{s1}} + \sqrt{L \cdot \cos\beta_{s1} \cdot \tan\beta_{s2}}} \tag{55}$$

$$L = \frac{2}{3} \cdot \xi^2 \cdot \eta \tag{56}$$

For ξ and η, see Figure 7 or Formulae (58) to (61) according to Reference [13].

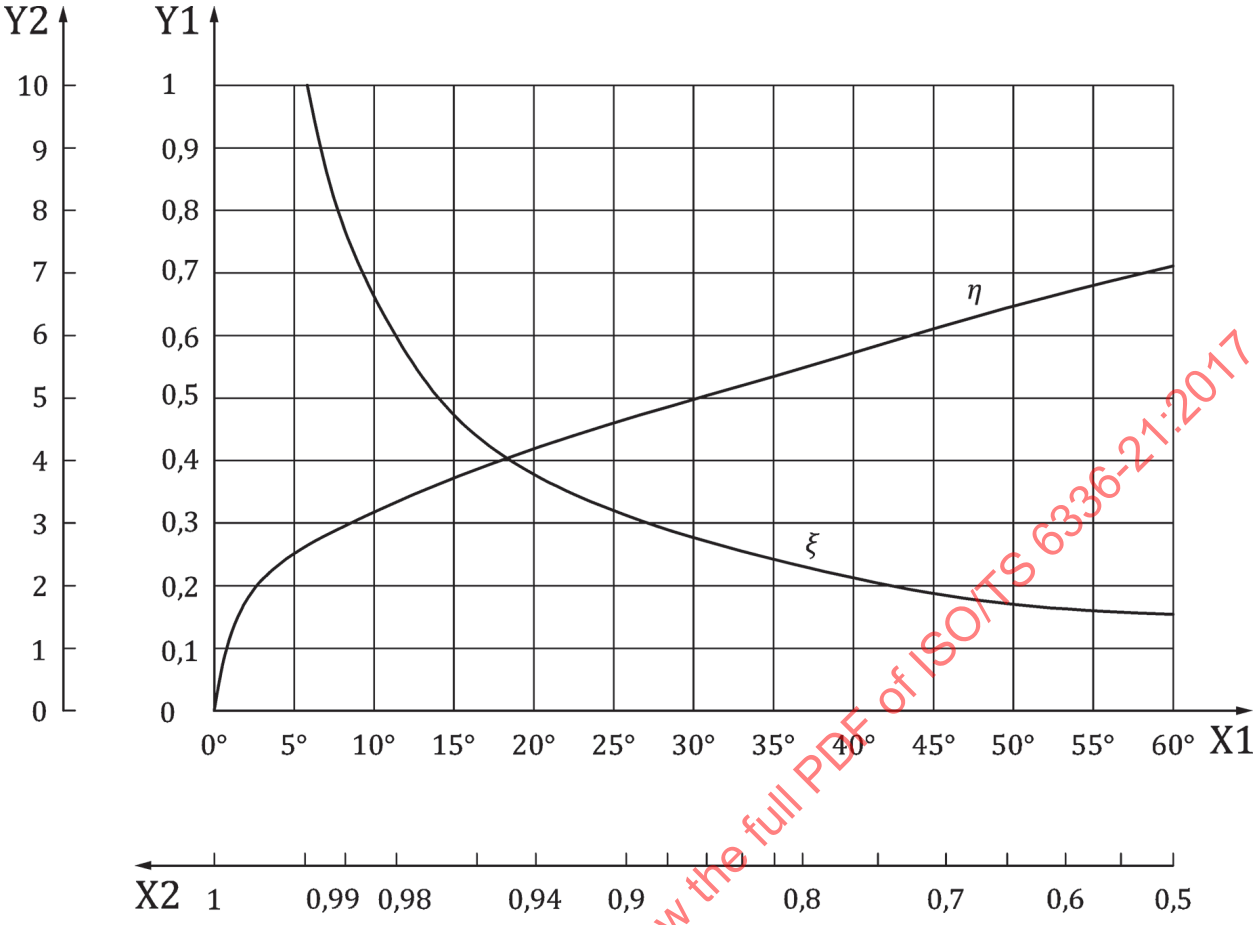

Key

X1 Herztian auxiliary angle, ϑ
X2 $\cos\vartheta$
Y1 Herztian auxiliary coefficient, η
Y2 Herztian auxiliary coefficient, ζ

Figure 7 — The auxiliary coefficients *x* and *h* as a function of $\cos\vartheta$

$$\cos\vartheta = \rho_{Cn}\sqrt{\frac{1}{\rho_{n1}^2}+\frac{1}{\rho_{n2}^2}+\frac{2\cdot\cos 2\varphi}{\rho_{n1}\cdot\rho_{n2}}} \tag{57}$$

For $0 \le \cos\vartheta < 0{,}949$, see Formula (58) and (59):

$$\ln\xi = \frac{\ln(1-\cos\vartheta)}{-1{,}53+0{,}333\cdot\ln(1-\cos\vartheta)+0{,}046\,7\cdot\left[\ln(1-\cos\vartheta)\right]^2} \tag{58}$$

$$\ln\eta = \frac{\ln(1-\cos\vartheta)}{1{,}525-0{,}86\cdot\ln(1-\cos\vartheta)-0{,}099\,3\cdot\left[\ln(1-\cos\vartheta)\right]^2} \tag{59}$$

For $0{,}949 \le \cos\vartheta < 1$, see Formula (60) and (61):

$$\ln\xi = \sqrt{-0{,}456\,7-0{,}444\,6\cdot\ln(1-\cos\vartheta)+0{,}123\,8\cdot\left[\ln(1-\cos\vartheta)\right]^2} \tag{60}$$

$$\ln\eta = -0{,}333+0{,}203\,7\cdot\ln(1-\cos\vartheta)+0{,}001\,2\cdot\left[\ln(1-\cos\vartheta)\right]^2 \tag{61}$$

6.3.9 Approach factor, X_Q

See 6.1.12, with the following substitutions:

— in Formulae (29) to (32): ε_{n1} instead of ε_1

ε_{n2} instead of ε

6.3.10 Tip relief factor, X_{Ca}

See 6.1.13, with the following substitution:

— in Formula (33): ε_{nmax} instead of ε_{max}

ε_{nmax} maximum value of ε_{n1} or ε_{n2}

For adequate tip and root relief,

$C_a/C_{eff} = 1$ (see 6.2.13).

6.3.11 Contact ratio factor, X_ε

$$X_\varepsilon = \frac{1}{\sqrt{\varepsilon_n}} \cdot \left[1 + 0{,}5 \cdot g^* \cdot \left(\frac{v_{g\gamma 1}}{v_{gs} - 1} \right) \right] \tag{62}$$

$$g^* = \frac{g_{an1}^2 + g_{an2}^2}{g_{an1}^2 + g_{an1} \cdot g_{an2}} \tag{63}$$

For gear pairs with about the same length of recess paths ($g_{an1} \approx g_{an2}$), the sliding factor g^* is close to unity.

6.3.12 Calculation of virtual crossed axes helical gears

This part contains geometrical relationships to convert a hypoid gear pair to a crossed axes helical gear pair. The conditions at mid-facewidth of hypoid gears are taken as basis for conversion (see Figure 8).

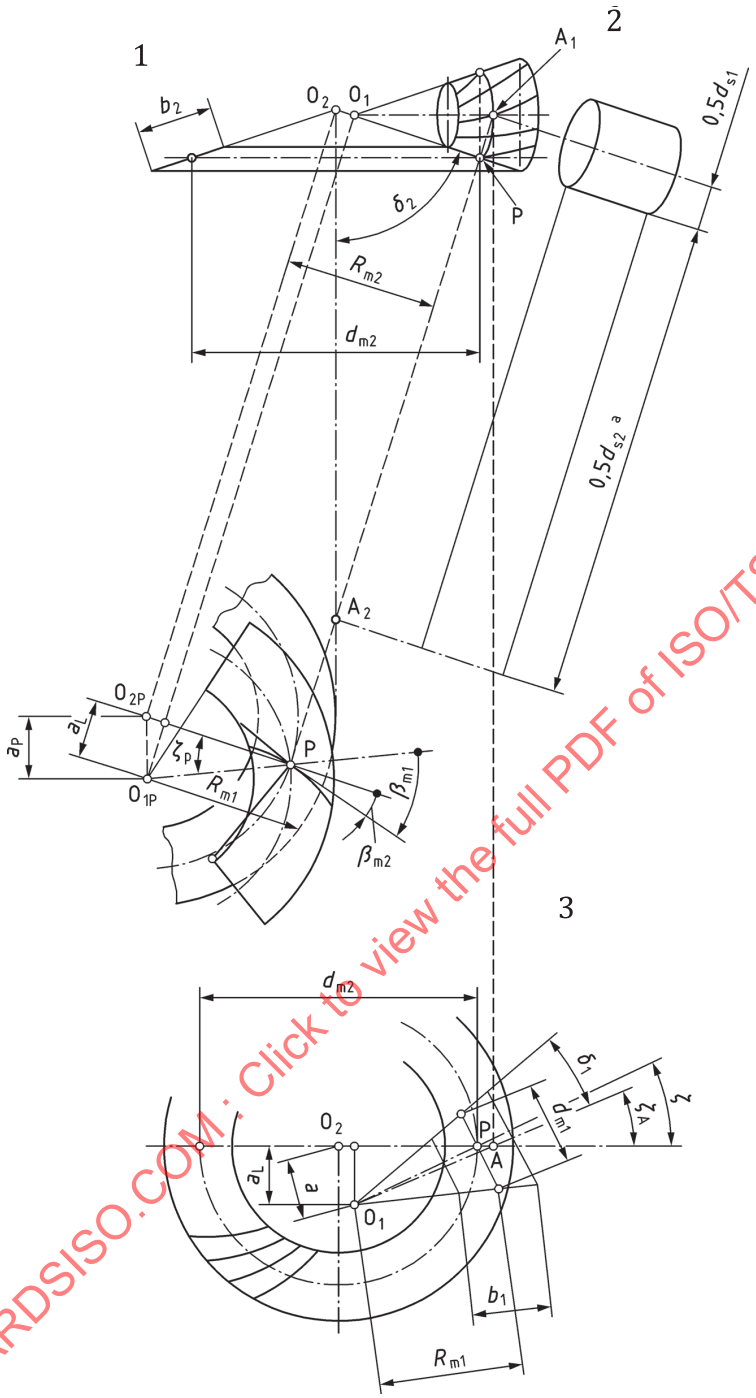

Key

1 hypoid gears
2 vertical view
3 plane view
a Mean virtual screwed helical gears.

Figure 8 — For the calculation of virtual crossed axes helical gears

Data of the virtual crossed axes helical gear:

Helix angle

$$\beta_{s1,2} = \beta_{m1,2} \tag{64}$$

Normal pressure angle

$$\alpha_{sn} = \alpha_{mn} \tag{65}$$

Crossing angle of crossed axes helical gear

$$\Sigma = \beta_{m1} - \beta_{m2} \tag{66}$$

Transverse pressure angle, $\alpha_{st1,2}$

$$\tan\alpha_{st1,2} = \frac{\tan\alpha_{sn}}{\cos\beta_{s1,2}} \tag{67}$$

Base helix angle, $\beta_{b1,2}$

$$\sin\beta_{b1,2} = \frac{\sin\beta_{s1,2}}{\cos\alpha_{sn}} \tag{68}$$

Reference circle

$$d_{s1,2} = \frac{d_{m1,2}}{\cos\delta_{1,2}} \tag{69}$$

Tip diameter

$$d_{a1,2} = d_{s1,2} + 2 \cdot h_{am1,2} \tag{70}$$

Base circle

$$d_{b1,2} = d_{s1,2} \cdot \cos\alpha_{t1,2} \tag{71}$$

Axle angle of crossed axes helical gear

$$\tan\beta_{b1,2} = \tan\beta_{m1,2} \cdot \sin\alpha_{mn} \tag{72}$$

$$\varphi = \beta_{b1} + \beta_{b2} \tag{73}$$

Module

$$m_{sn} = m_{mn} \tag{74}$$

Normal base pitch

$$p_{en} = m_{sn} \cdot \pi \cdot \cos\alpha_{sn} \tag{75}$$

Radii of curvature in normal section

$$\rho_{n1,2} = 0{,}5 \cdot d_{s1,2} \cdot \frac{\sin^2 \alpha_{t1,2}}{\sin \alpha_{sn}} \tag{76}$$

$$\rho_{Cn} = \frac{\rho_{n1} \cdot \rho_{n2}}{\rho_{n1} + \rho_{n2}} \tag{77}$$

Tangential velocities

$$v_{t1} = \frac{\pi \cdot n_1 \cdot d_{m1}}{60\,000} \tag{78}$$

$$v_{t2} = v_{t1} \cdot \frac{\cos \beta_{s1}}{\cos \beta_{s2}} \tag{79}$$

Sum of the tangential speeds at pitch point $v_{\Sigma C}$ (b_{s1}, b_{s2} positive)

$$v_{\Sigma s} = v_{tl} \left(\sin \beta_{s1} + \sin \beta_{s2} \cdot \frac{\cos \beta_{s1}}{\cos \beta_{s2}} \right) \tag{80}$$

$$v_{\Sigma h} = 2 v_{t1} \cos \beta_{s1} \sin \alpha_{sn} \tag{81}$$

$$v_{\Sigma C} = \sqrt{v_{\Sigma s}^2 + v_{\Sigma h}^2} \tag{82}$$

Sliding velocity at pitch point

$$v_{gs} = v_{t1} \cdot \frac{\sin \Sigma}{\cos \beta_{s2}} \tag{83}$$

Maximum sliding velocity at tip of pinion $v_{g\gamma 1}$

$$v_{g\gamma 1} = \sqrt{v_{g\alpha 1}^2 + v_{g\beta 1}^2} \tag{84}$$

$$v_{g1} = 2 \cdot v_{t1} \cdot g_{an1} \cdot \frac{\cos \beta_{b1}}{d_{s1}} \tag{85}$$

$$v_{g2} = 2 \cdot v_{t2} \cdot g_{an2} \cdot \frac{\cos \beta_{b2}}{d_{s2}} \tag{86}$$

$\gamma_{1,2}$ from $\tan \gamma_{1,2} = \sin \alpha_{sn} \cdot \tan \beta_{s1,2}$ (87)

$$v_{g\alpha 1} = v_{g1} \cdot \cos \gamma_1 + v_{g2} \cdot \cos \gamma_2 \tag{88}$$

$$v_{g\beta 1} = v_{gs} + v_{g1} \cdot \sin \gamma_1 - v_{g2} \cdot \sin \gamma_2 \tag{89}$$

Path of contact

$$\overline{AE} = g_{an1} + g_{an2} \tag{90}$$

$$g_{an1} = \frac{g_{at1}}{\cos\beta_{b1}} = \frac{0{,}5\left(\sqrt{d_{a1}^2 - d_{b1}^2} - \sqrt{d_{s1}^2 - d_{b1}^2}\right)}{\cos\beta_{b1}} = \overline{SE} = g_{fn2} \tag{91}$$

$$g_{an2} = \frac{0{,}5 \cdot \left(\sqrt{d_{a2}^2 - d_{b2}^2} - \sqrt{d_{s2}^2 - d_{b2}^2}\right)}{\cos\beta_{b2}} = \overline{SA} = g_{fn1} \tag{92}$$

Contact ratio in normal section

$$\varepsilon_n = \frac{\overline{AE}}{p_{en}} \tag{93}$$

$$\varepsilon_{n1,2} = \frac{g_{an1,2}}{p_{en}} \tag{94}$$

6.4 Scuffing integral temperature

6.4.1 General

The scuffing integral temperature is the limiting value of the temperature at which scuffing occurs. It can be calculated on the basis of test results.

This method is valid for all types of oils (pure mineral oils, EP-oils, synthetic oils) for which the scuffing load capacity has been determined in a test gear (suitable tests are, for example, the FZG-test A/8,3/90, the FZG L-42 test, the Ryder gear oil test or the IAE gear oil test), or by an actual case of damage.

The scuffing temperature shall be corrected when material and heat treatment of the test gear are not identical with that of the actual gear, as the limiting temperature is a function of the material-oil system.

6.4.2 Scuffing integral temperature, ϑ_{intS}

6.4.2.1 General

According to the integral temperature postulate, gears are likely to scuff when the mean flank temperature exceeds a value termed the scuffing integral temperature number. This number is assumed to be characteristic for the lubricant and gear material combination of a gear pair and is to be determined by testing a similar lubricant and gear material combination.

A scuffing integral temperature number can be derived from the results of any gear oil scuffing test by entering the test data into the formulae in 6.1, 6.2, 6.3. Thus, scuffing integral temperature numbers for any oil, straight mineral, EP or synthetic, can be evaluated.

6.4.2.2 Calculation of the scuffing integral temperature

The approximate scuffing integral temperature number of heat or surface-treated gear steels in combination with a mineral oil, can be derived from that of a combination of gear steels with other heat or surface treatments and the same lubricant.

$$\vartheta_{intS} = \vartheta_{MT} + X_{WrelT} \cdot C_2 \cdot \vartheta_{flaintT} \tag{95}$$

where C_2 = 1,5; derived from experiments.

6.4.2.3 Determination of ϑ_{MT}, $\vartheta_{flaintT}$ from test results

Figure 9 shows the diagram for mineral oils in case that the scuffing load capacity is determined in an FZG-Test A/8,3/90 in accordance with DIN 51354[5], in a Ryder[6] or an FZG-Ryder test[7] and in an FZG L-42 test[8].

For computer calculations the diagrams in Figures 9 to 11 can be approximated by the following formulae:

a) For the FZG test A/8,3/90:

$$\vartheta_{MT} = 80 + 0{,}23 \cdot T_{1T} \cdot X_L \tag{96}$$

$$\vartheta_{flaintT} = 0{,}2 \cdot T_{1T} \cdot \left(\frac{100}{ny_{40}} \right)^{0{,}02} \cdot X_L \tag{97}$$

$$T_{1T} = 3{,}726 \cdot (\text{FZG load stage})^2 \tag{98}$$

b) For the Ryder and the FZG-Ryder test R/46,5/74:

$$\vartheta_{MT} = 90 + 0{,}012\,5 \left(\frac{F_{bt}}{b} \right)_T \cdot X_L \tag{99}$$

with F_{bt}/b in lb/in.

c) For the FZG L-42 test 141/19,5/110:

$$\vartheta_{MT} = 110 + 0{,}02 \cdot T_{1T} \cdot X_L \tag{100}$$

$$\vartheta_{flaintT} = 0{,}48 \cdot T_{1T} \cdot \left(\frac{100}{ny_{40}} \right)^{0{,}02} \cdot X_L \tag{101}$$

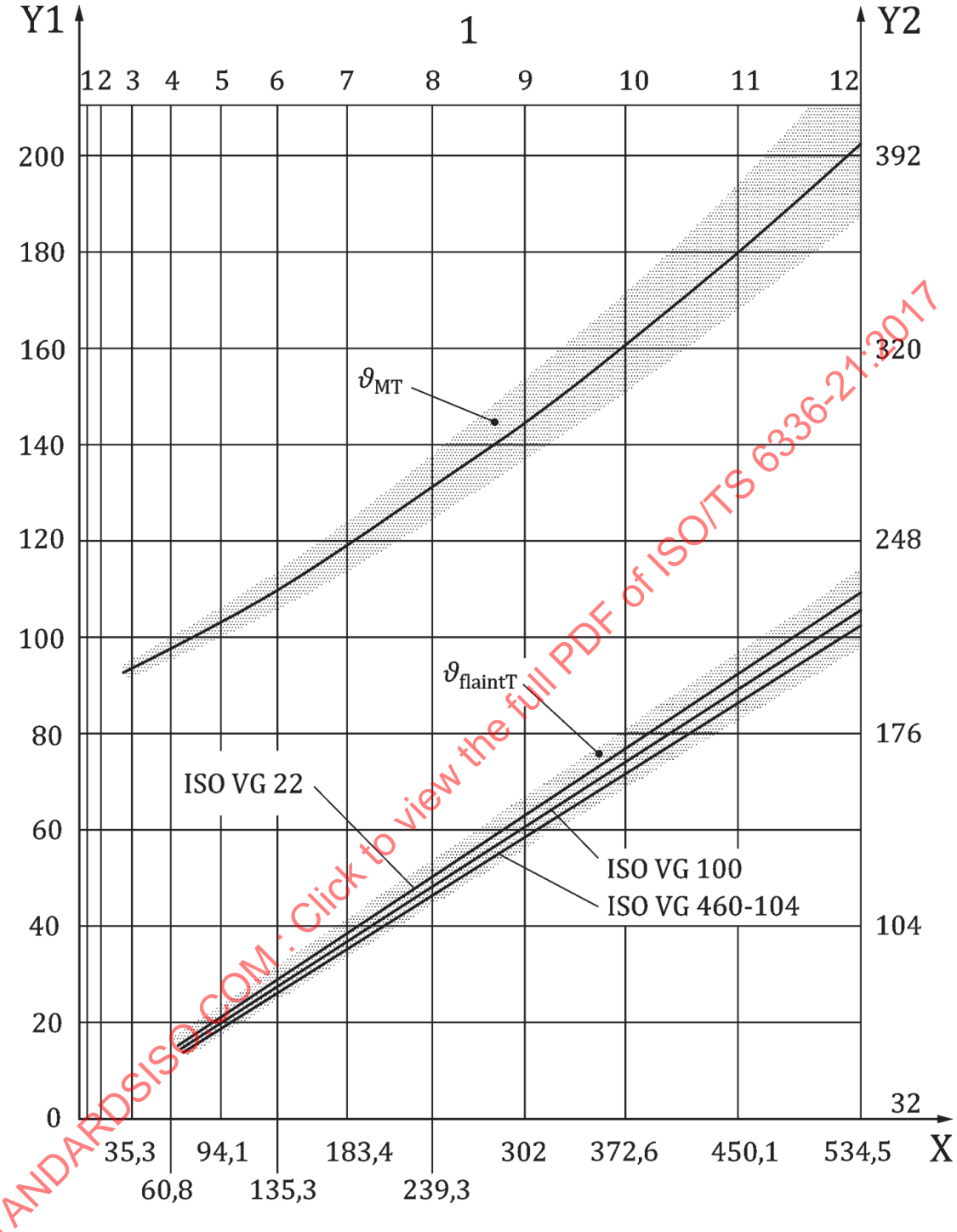

Key

1 load stages FZG-test
X pinion test torque T_{1T}, N·m
Y1 temperature, in °C
Y2 temperature, in °F

Figure 9 — Scuffing temperature, ϑ_{intS}, for the FZG test A/8,3/90

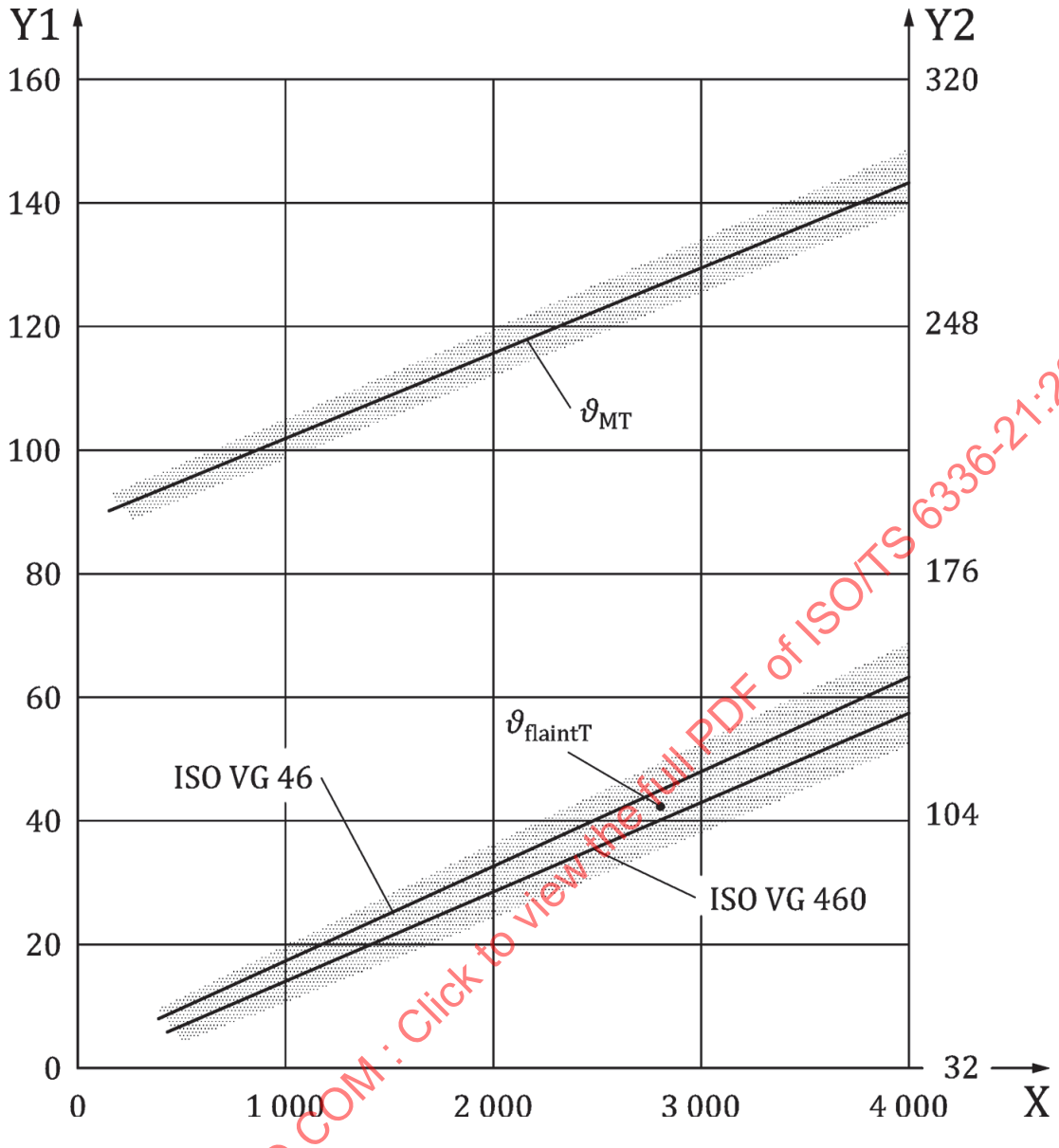

Key

X normal load per face width, $(F_{bt}/b)_T$, in ppi

Y1 temperature, in °C

Y2 temperature, in °F

Figure 10 — Scuffing temperature, ϑ_{intS}, for the Ryder and the FZG-Ryder gear test R/46,5/74

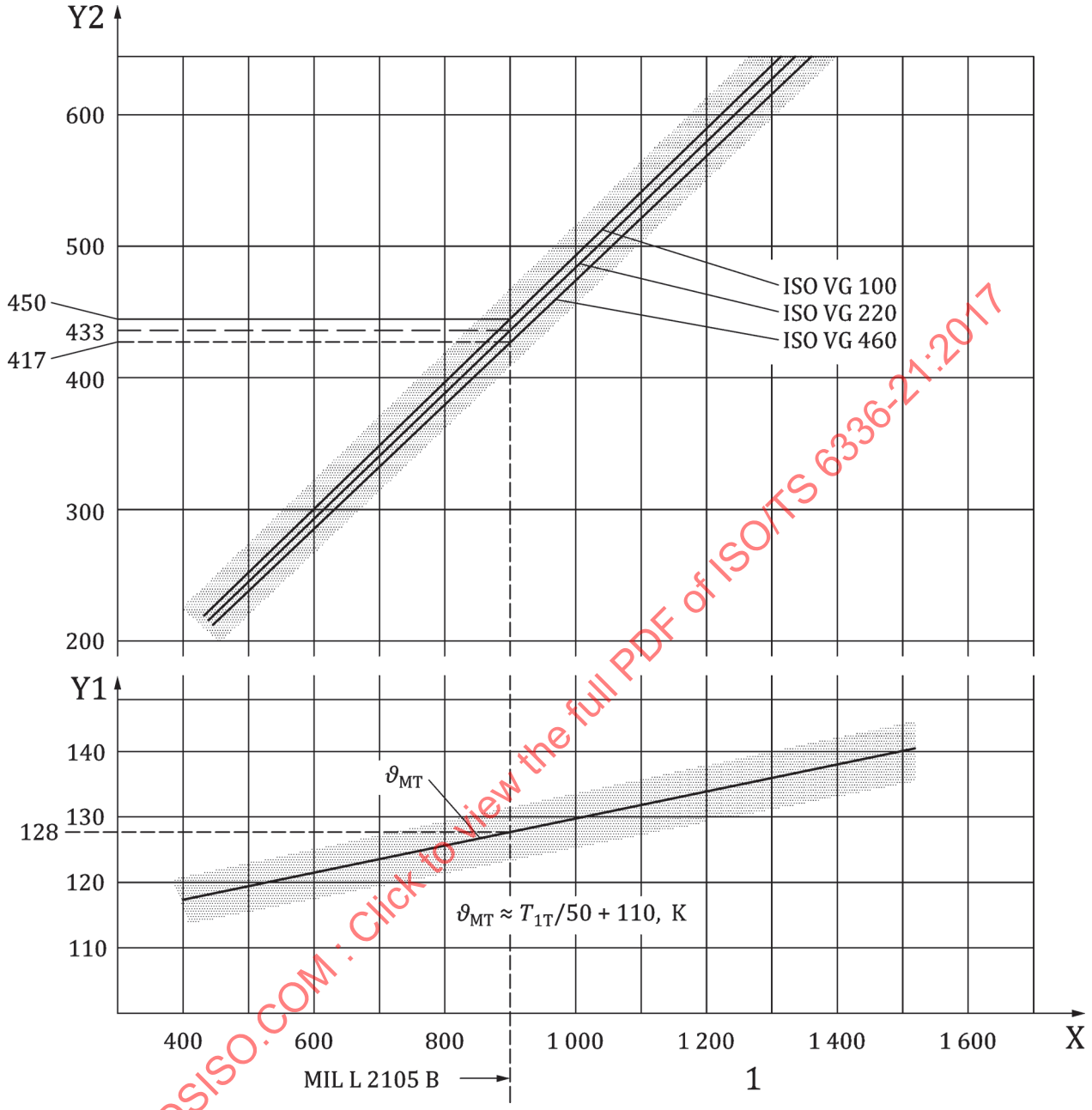

Key

1 test torque of pinion

X scuffing torque of test pinion T_{1T}, in N·m

Y1 test bulk temperature, ϑ_{MT}, in K

Y2 mean flash temperature of the test gear, $\vartheta_{flaintT}$, in K

NOTE $\vartheta_{flaintT} \approx 0{,}75\, T_{1T}{}^{0,95}\, \eta_{MT}{}^{-0,05}$, K

Approximation

$$\eta_{MT} \approx \eta_{40}\left(40 / \vartheta_{MT}\right)^{2,85}$$

Figure 11 — Scuffing temperature, ϑ_{intS}, for the FZG L-42 test 141/19,5/110

6.4.3 Relative welding factor, X_{WrelT}

The relative welding factor, X_{WrelT}, is an empirical factor for the influence of the heat or surface treatment on the scuffing integral temperature, as shown in Formula (102):

$$X_{WrelT} = \frac{X_W}{X_{WT}} \tag{102}$$

where

X_{WT} is 1 for the FZG gear test, the Ryder gear test and the FZG L-42 test;

X_W is the welding factor of the actual gear material as given in Table 4.

Table 4 — Welding factor, X_W

Gear material	X_W
Through-hardened steel	1,00
Phosphated steel	1,25
Copper-plated steel	1,50
Bath and gas nitrided steel	1,50
Case carburized steel:	
— average austenite content less than 10 %	1,15
— average austenite content 10 % to 20 %	1,00
— average austenite content greater than 20 % to 30 %	0,85
Austenitic steel (stainless steel)	0,45

Annex A
(informative)

Examples

Verifying the accuracy of the integral temperature method, the scuffing resistance of the following gear sets was calculated by using the methods according to this document. The examples contain cylindrical, bevel and hypoid gear drives, with centre distances between a = 22,07 mm and a = 2 419,63 mm. The module range includes modules from m = 1,25 mm up to m = 20 mm. Some of the selected gear units were damaged by a scuffing failure, or near to the scuffing limit (borderline scuffing). In other gear drives, no scuffing failure was observed. The data of the gear units and the results of the scuffing calculation are presented in the following tables.

Table A.1 — Helical gear: Turbine Gear (No. 3 from the Michaelis dissertation)

Description		ISO symbol	Unit	Value
Number of teeth	pinion	z_1	—	73
	gear	z_2	—	325
Operating centre distance		a	mm	1 419,00
Normal module		m_n	mm	7,000
Normal pressure angle		α_n	°	20,00
Helix angle at standard PD		β	°	11,00
Profile shift factor	pinion	x_1	—	0,010 0
Net face width		b	mm	280,00
Outside diameter	pinion	d_{a1}	mm	534,40
	gear	d_{a2}	mm	2 331,00
Tip relief	pinion	C_{a1}	µm	0
	gear	C_{a2}	µm	0
Index of driving gear		—	—	2
Transmitted power		P	kW	10 295
Pinion speed		n_1	min^{-1}	4 450
Flank surface roughness		R_a	µm	2,00
Tooth root surface roughness		R_z	µm	-
Oil temperature		ϑ_{oil}	°C	40
Lubricant kinematic viscosity at 40 °C		v_{40}	mm^2/s	32
Scuffing torque in FZG standard test A/8,3/90 according to DIN 51354		T_{1T}	Nm	239
Lubrication factor		X_S	—	1,2
Relative material factor		X_{WrelT}	—	1,00
Run-in factor		X_E	—	1,0
Application factor		K_A	—	1,20
Dynamic factor		K_v	—	1,15
Face load factor		$K_{B\beta}$	—	1,20
Transverse load factor		$K_{B\alpha}$	—	1,10
Coefficient of friction		μ_{mC}	—	0,023

Table A.1 *(continued)*

Description	ISO symbol	Unit	Value
Bulk temperature	ϑ_M	°C	45,6
Integral temperature	ϑ_{int}	°C	55,5
Scuffing safety factor	S_{intS}	—	3,8
Observed failures	No scuffing		

Table A.2 — Helical gear: Steel Mill Gear (No. 5 from the Michaelis dissertation)

Description		ISO symbol	Unit	Value
Number of teeth	pinion	z_1	—	28
	gear	z_2	—	28
Operating centre distance		a	mm	580,00
Normal module		m_n	mm	20,000
Normal pressure angle		α_n	°	20,00
Helix angle at standard PD		β	°	10,00
Profile shift factor	pinion	x_1	—	0,303 5
Net face width		b	mm	330,00
Outside diameter	pinion	d_{a1}	mm	619,20
	gear	d_{a2}	mm	619,20
Tip relief	pinion	C_{a1}	µm	0
	gear	C_{a2}	µm	0
Index of driving gear		—	—	1
Transmitted power		P	kW	2 200
Pinion speed		n_1	min^{-1}	150
Flank surface roughness		R_a	µm	1,50
Tooth root surface roughness		R_z	µm	-
Oil temperature		ϑ_{oil}	°C	32
Lubricant kinematic viscosity at 40 °C		v_{40}	mm^2/s	220
Scuffing torque in FZG standard test A/8,3/90 according to DIN 51354		T_{1T}	Nm	239
Lubrication factor		X_S	—	1,2
Relative material factor		X_{WrelT}	—	1,00
Run-in factor		X_E	—	1,0
Application factor		K_A	—	1,20
Dynamic factor		K_v	—	1,00
Face load factor		$K_{B\beta}$	—	1,20
Transverse load factor		$K_{B\alpha}$	—	1,00
Coefficient of friction		μ_{mC}	—	0,048
Bulk temperature		ϑ_M	°C	59,6
Integral temperature		ϑ_{int}	°C	109,0
Scuffing safety factor		S_{intS}	—	1,9
Observed failures		No scuffing		

Table A.3 — Helical gear: Machine Tool Gear (No. 11 from the Michaelis dissertation)

Description		ISO symbol	Unit	Value
Number of teeth	pinion	z_1	—	5
	gear	z_2	—	28
Operating centre distance		a	mm	22,07
Normal module		m_n	mm	1,250
Normal pressure angle		α_n	°	20,00
Helix angle at standard PD		β	°	20,00
Profile shift factor	pinion	x_1	—	0,350 0
Net face width		b	mm	10,00
Outside diameter	pinion	d_{a1}	mm	9,98
	gear	d_{a2}	mm	38,45
Tip relief	pinion	C_{a1}	µm	0
	gear	C_{a2}	µm	0
Index of driving gear		—	—	1
Transmitted power		P	kW	3,3
Pinion speed		n_1	min^{-1}	15 000
Flank surface roughness		R_a	µm	1,00
Tooth root surface roughness		R_z	µm	—
Oil temperature		ϑ_{oil}	°C	50
Lubricant kinematic viscosity at 40 °C		v_{40}	mm^2/s	220
Scuffing torque in FZG standard test A/8,3/90 according to DIN 51354		T_{1T}	Nm	450
Lubrication factor		X_S	—	1,0
Relative material factor		X_{WrelT}	—	1,00
Run-in factor		X_E	—	1,0
Application factor		K_A	—	1,00
Dynamic factor		K_v	—	1,00
Face load factor		$K_{B\beta}$	—	1,00
Transverse load factor		$K_{B\alpha}$	—	1,00
Coefficient of friction		μ_{mC}	—	0,144
Bulk temperature		ϑ_M	°C	84,8
Integral temperature		ϑ_{int}	°C	159,4
Scuffing safety factor		S_{intS}	—	2,0
Observed failures		No scuffing		

Table A.4 — Helical gear: Marine Gear (No. 13 from the Michaelis dissertation)

Description		ISO symbol	Unit	Value
Number of teeth	pinion	z_1	—	21
	gear	z_2	—	87
Operating centre distance		a	mm	900,00
Normal module		m_n	mm	16,00
Normal pressure angle		α_n	°	20,00
Helix angle at standard PD		β	°	10,00
Profile shift factor	pinion	x_1	—	0,790 0
Net face width		b	mm	370,00
Outside diameter	pinion	d_{a1}	mm	394,50
	gear	d_{a2}	mm	1 465,50
Tip relief	pinion	C_{a1}	µm	0
	gear	C_{a2}	µm	0
Index of driving gear		—	—	1
Transmitted power		P	kW	4 412
Pinion speed		n_1	min^{-1}	520
Flank surface roughness		R_a	µm	2,00
Tooth root surface roughness		R_z	µm	—
Oil temperature		ϑ_{oil}	°C	60
Lubricant kinematic viscosity at 40 °C		v_{40}	mm^2/s	150
Scuffing torque in FZG standard test A/8,3/90 according to DIN 51354		T_{1T}	Nm	450
Lubrication factor		X_S	—	1,2
Relative material factor		X_{WrelT}	—	1,00
Run-in factor		X_E	—	1,0
Application factor		K_A	—	1,30
Dynamic factor		K_v	—	1,05
Face load factor		$K_{B\beta}$	—	1,40
Transverse load factor		$K_{B\alpha}$	—	1,00
Coefficient of friction		μ_{mC}	—	0,058
Bulk temperature		ϑ_M	°C	105,1
Integral temperature		ϑ_{int}	°C	185,7
Scuffing safety factor		S_{intS}	—	1,7
Observed failures		Borderline scuffing		